JAERI-M
91-169

NEOCLASSICAL TRANSPORT ANALYSIS OF TITANIUM IMPURITY IN PLASMAS WITH STRONGLY PEAKED DENSITY PROFILES

October 1991

Toshio HIRAYAMA, Tatsuo SUGIE, Akira SAKASAI
Ryuuji YOSHINO and Yutaka KAMADA

日本原子力研究所
Japan Atomic Energy Research Institute

JAERI-Mレポートは，日本原子力研究所が不定期に公刊している研究報告書です。
入手の問合わせは，日本原子力研究所技術情報部情報資料課（〒319-11 茨城県那珂郡東海村）あて，お申しこみください。なお，このほかに財団法人原子力弘済会資料センター（〒319-11 茨城県那珂郡東海村日本原子力研究所内）で複写による実費領布をおこなっております。

JAERI-M reports are issued irregularly.
Inquiries about availability of the reports should be addressed to Information Division Department of Technical Information, Japan Atomic Energy Research Institute, Tokaimura, Naka-gun, Ibaraki-ken 319-11, Japan.

編集兼発行　日本原子力研究所
印　　刷　ニッセイエブロ株式会社

JAERI-M 91-169

Neoclassical Transport Analysis of Titanium Impurity in Plasmas with Strongly Peaked Density Profiles

Toshio HIRAYAMA, Tatsuo SUGIE, Akira SAKASAI
Ryuuji YOSHINO and Yutaka KAMADA

Department of Fusion Plasma Research
Naka Fusion Research Establishment
Japan Atomic Energy Research Institute
Naka-machi, Naka-gun, Ibaraki-ken

(Received September 20, 1991)

The full neoclassical multi-ion calculation required for the interaction between titanium and light impurities like carbon and oxygen is presented. Intrinsic titanium impurity behavior in pellet fuelled plasmas was studied by applying the neoclassical impurity transport calculation to temporal evolutions of Ti XX and Ti XXI spectroscopically observed. Ti impurity accumulates in the plasma core region, correlated with peaked density profile and the absence of sawtooth oscillation. Impurity accumulation is caused by a strong ion density gradient driving force and collisions with light impurities, as the neoclassical impurity transport theory predicts. This impurity behavior is well described by the combination of reduced anomalous diffusion and neoclassical transport in the plasma interior. The reduced anomalous diffusion at the central region inside the q=1 is estimated to be 0.2 m^2/s. The outer zones continue to be dominated by anomalous transport.

Keywords: Tokamak, Plasma, Pellet, Neoclassical Impurity Transport, Impurity Accumulation

JAERI－M 91－169

急峻な密度勾配を有するプラズマ中のチタン不純物の新古典理論輸送解析

日本原子力研究所那珂研究所炉心プラズマ研究部
平山　俊雄・杉江　達夫・逆井　章・芳野　隆治・鎌田　裕

（1991年9月20日受理）

ペレット入射により形成された急峻な密度勾配を有するプラズマについて，新古典輸送理論に基づく不純物輸送計算結果を，実験的に得られたＴｉＸＸ及びＴｉＸＸＩのスペクトル線の時間変化と比較することによりチタン不純物の輸送特性を調べた。チタン不純物は，急峻な密度分布と鋸歯状波振動の抑制に関連して，プラズマ中心領域に集注する。チタン不純物の挙動は，プラズマ内部での異常輸送の低減と新古典輸送モデルにより説明できる。この不純物の中心集中は，新古典不純物輸送理論が予測するように，強い密度勾配と軽元素不純物との衝突により生じる。低減した異常輸送係数は，q＝1面内の中心領域では，0.2 ㎡/sと推定できる。プラズマ周辺領域はなお，異常輸送が支配的である。

那珂研究所：〒311－01　茨城県那珂郡那珂町大字向山801－1

Contents

1. Introduction 1
2. Neoclassical Flux of Impurity Ions 1
3. Intrinsic Titanium Impurity Behavior in Pellet Fueled Plasmas . 5
4. Unsteady Impurity Transport Analysis 6
5. Summary and Discussion 8
Acknowledgment 9
References 9

目　　次

1. 序　論 1
2. 不純物イオンの新古典粒子束 1
3. ペレットプラズマ中のチタン不純物の挙動 5
4. 非定常不純物輸送解析 6
5. 結　言 8
謝　辞 9
参考文献 9

1. Introduction

It is well known that transport processes in tokamaks have generally been found to be anomalous. However, the most interesting aspect of impurity transport is the often observed correlation between long impurity particle confinement and improved energy confinement. This result has been seen in discharges exhibiting transport changes. In JT-60[1], improved energy confinement for additionally heated, limiter and lower x-point discharges has been obtained with hydrogen pellet injection. The temporal evolutions of Ti XIX, XX and XXI emissivity lines have dynamically changed following the injection of frozen hydrogen pellets. These behaviors will be able to be explained approximately by neoclassical models. In view of this, we describe calculations of the predicted temporal evolutions of titanium impurity ions in JT-60 using the neoclassical theory. Indeed, the study of impurities in tokamaks provides excellent opportunities to measure transport coefficients. Since individual impurities are readily identifiable through their characteristic line radiation, it is possible to follow the spatial and temporal evolution of ion densities.

The full neoclassical multi-ion impurity flux required for the interaction between heavy and light impurities is presented in Section 2. The impurity behavior in pellet fuelled plasmas with improved energy confinement and the transport analysis of Ti impurity are described in Sections 3 and 4, respectively. Finally, the main results are summarized in Section 5.

2. Neoclassical flux of impurity ions

The transport of impurity ions can be described by the simple expression of particle conservation

$$\frac{\partial n_k}{\partial t} = -\frac{1}{r}\frac{\partial}{\partial r} r\Gamma_k - \frac{n_k}{\tau_{//}} + S_k \qquad (1)$$

where n_k is the impurity ion density with the k-th charge state, Γ_k the flux of ions across the magnetic flux surfaces, $n_k/\tau_{//}$ the loss term along the magnetic lines in the scrape-off

1. Introduction

It is well known that transport processes in tokamaks have generally been found to be anomalous. However, the most interesting aspect of impurity transport is the often observed correlation between long impurity particle confinement and improved energy confinement. This result has been seen in discharges exhibiting transport changes. In JT-60[1], improved energy confinement for additionally heated, limiter and lower x-point discharges has been obtained with hydrogen pellet injection. The temporal evolutions of Ti XIX, XX and XXI emissivity lines have dynamically changed following the injection of frozen hydrogen pellets. These behaviors will be able to be explained approximately by neoclassical models. In view of this, we describe calculations of the predicted temporal evolutions of titanium impurity ions in JT-60 using the neoclassical theory. Indeed, the study of impurities in tokamaks provides excellent opportunities to measure transport coefficients. Since individual impurities are readily identifiable through their characteristic line radiation, it is possible to follow the spatial and temporal evolution of ion densities.

The full neoclassical multi-ion impurity flux required for the interaction between heavy and light impurities is presented in Section 2. The impurity behavior in pellet fuelled plasmas with improved energy confinement and the transport analysis of Ti impurity are described in Sections 3 and 4, respectively. Finally, the main results are summarized in Section 5.

2. Neoclassical flux of impurity ions

The transport of impurity ions can be described by the simple expression of particle conservation

$$\frac{\partial n_k}{\partial t} = -\frac{1}{r}\frac{\partial}{\partial r} r\Gamma_k - \frac{n_k}{\tau_{//}} + S_k \qquad (1)$$

where n_k is the impurity ion density with the k-th charge state, Γ_k the flux of ions across the magnetic flux surfaces, $n_k/\tau_{//}$ the loss term along the magnetic lines in the scrape-off

layer and S_k the source term consisting of the ionization and recombination. The particle flux of an impurity ion is given by a combination of the anomalous and neoclassical transport fluxes

$$\Gamma_k = \Gamma_k^A + \Gamma_k^{NC} \tag{2}$$

where Γ_k^A is the anomalous flux and Γ_k^{NC} the neoclassical flux. The conventional approach assumes the impurity anomalous flux Γ_k^A to be given by

$$\Gamma_k^A(r) = -D_A(r)\frac{\partial n_k}{\partial r} + V_A(r)n_k \tag{3}$$

where n_k is the impurity ion density in the k-th charge state, $D_A(r)$ an anomalous diffusion coefficient and $V_A(r)$ an anomalous convective velocity. From the diffusive/convective model[2], the convective velocity is related to the anomalous diffusion coefficient through a form such as

$$V_A(r) = -C_V D_A \frac{2r}{r_p^2} \tag{4}$$

where C_V is a dimensionless peaking parameter. When $C_V = 1$, Equation (3) provides a gaussian profile of impurity ion density at steady state. Higher values of C_V lead to more peaked density profiles. The diffusion coefficient D_A and the peaking parameter C_V are to be determined from the simulations and are assumed to be the same for all ionization states. Following a previous analysis of Ti impurity in NB heated, L-mode plasmas[3], we take D_A to be spatially uniform and its value to be $1.0\ m^2/s$.

In the following discussion, we will be concerned with the study of the impurity transport alone in high density plasmas fueled by hydrogen pellets. In order to provide a framework for this, let us consider the Pfirsch-Schluter flux of an impurity driven by friction against several working ion species. From the neoclassical theory[4], the Pfirsch-Schluter flux of an impurity for a collision with one main ion can be written in the general form

$$\Gamma_k^{PS} = n_k D_k \left[- L_k \frac{n_k'}{n_k} + \frac{eZ_k}{T_k} (E_r - B_\theta U_{11}) + H_k \frac{T_k'}{T_k} \right] \tag{5}$$

where

$$D_k = q^2 \rho_k^2 \sum_{j \neq k} \nu_{kj}, \tag{6}$$

$$L_k = 1 - \frac{3}{7} P_k , \tag{7}$$

$$H_k = \frac{L_k}{2} - \frac{12}{35} \left(1 + \frac{1}{\sqrt{2}\Delta_k}\right) P_k , \tag{8}$$

$$P_k = \frac{2.062 \Delta_k g_k^2}{9.035 + (1 + 1.701\Delta_k) g_k^2} , \tag{9}$$

$$g_k = \frac{\nu_{*2}^{ik}}{\Delta_k} , \text{ and } \Delta_k = \frac{n_k}{n_i} \left(\frac{Z_k}{Z_i}\right)^2 .$$

The prime ' means the spatial derivative. The larmor radius, ρ_k is given by

$$\rho_k = \frac{\sqrt{2 m_k \kappa T_k}}{Z_k e B_z} . \tag{10}$$

The collision frequency, ν_{ki} is given in the general form

$$\nu_{ki} = \frac{4 (2\pi)^{1/2} e^4}{3 (4\pi\varepsilon_0)^2 \kappa^{3/2}} \frac{m_{ki}^{1/2} Z_k^2 Z_i^2 n_k n_i \ln\Lambda_{ki}}{m_k T_{ki}^{3/2}} \tag{11}$$

where

$$\Lambda_{ki} = \frac{3(4\pi\varepsilon_0\kappa)^{3/2}}{2\sqrt{\pi} Z_k Z_i e^3} \left\{ \frac{T_e T_i}{(Z_{eff} T_e + T_i) n_e} \right\}^{1/2} T_{ki} , \tag{12}$$

$$m_{ki} = \frac{m_k m_i}{m_k + m_i} \text{ and } T_{ki} = \frac{m_k T_i + m_i T_k}{m_k + m_i} .$$

The coefficient, L_k of n_k'/n_k in Γ_k^{PS} decreases from 1.0 to somewhat below unity as the collisionality increases. The coefficient H_k of T_k'/T_k decreases rapidly from 0.5 to zero across the intermediate Pfirsch-Schluter regime and is negative (~ -0.1) over the extreme Pfirsch-Schluter regime. The values of the coefficients L_k and H_k given by Eqns (7), (8) and (9) are valid only if the main ions are in the Pfirsch-Schluter regime. However, even if the main ions are in the banana regime or in the plateau regime, the impurity ion flux is given as the Pfirsch-Schluter-like formula of Eqn (5), taking for the coefficients L_k and H_k the values of 1.0 and 0.5, respectively [4]. To evaluate the fluxes due to collisions between the background plasma and impurity ions as well as to collisions between various ionization states, we must first find the poloidal rotation from the ambipolar condition, $\sum Z_j\Gamma_j = 0$. This gives

$$(E_r - B_\theta U_{11}) \sum \frac{eZ_j^2 D_j n_j}{T_j} = \sum Z_j D_j n_j \left[L_j \frac{n_j'}{n_j} - H_j \frac{T_j'}{T_j} \right] \tag{13}$$

where the electron flux is $O(m_e/m_i)^{1/2}$ and can be neglected. Using Eqn (10), we can eliminate $(E_r - B_\theta U_{11})$ from Eqn (5) and obtain the simplified equation for the flux driven by friction against several working ion species,

$$\Gamma_k^{PS} = n_k D_k \left[- L_k \frac{n_k'}{n_k} + H_k \frac{T_k'}{T_k} + \frac{eZ_k}{T_k} \sum Z_j D_j n_j \left\{ L_j \frac{n_j'}{n_j} - H_j \frac{T_j'}{T_j} \right\} / \sum \frac{eZ_j^2 D_j n_j}{T_j} \right] \tag{14}$$

Therefore, the neoclassical flux of an impurity ion is approximated to be, including the classical flux,

$$\Gamma_k^{NC} = \Gamma_k^{cl} + \Gamma_k^{PS}$$

$$= n_k D_k^{NC} \left[- L_k \frac{n_k'}{n_k} + H_k \frac{T_k'}{T_k} + \frac{eZ_k}{T_k} \sum Z_j D_j n_j \left\{ L_j \frac{n_j'}{n_j} - H_j \frac{T_j'}{T_j} \right\} / \sum \frac{eZ_j^2 D_j n_j}{T_j} \right] \tag{15}$$

where $D_k^{NC} = \left(\frac{1}{2} + q^2 \right) \rho_k^2 \sum_{j \neq k} \nu_{kj}$.

Using the above combination of neoclassical and anomalous transport fluxes, a one-dimensional and time dependent, multi-species impurity code[5] is employed to calculate the impurity ion density and the emissivity lines, in pellet fueled plasmas.

3. Intrinsic titanium impurity behavior in pellet fueled plasmas

Centrally peaked electron density profiles lasting for one second were obtained by injection of four hydrogen pellets into JT-60 neutral beam heated discharges. A four-barrel pneumatic pellet injector installed on JT-60 produces cylindrical hydrogen pellets with velocities approaching 1.6 km/s. The pellet sizes are 2.7 mm (dia.) × 2.7 mm (length) and 3.8 mm (dia.) × 3.8 mm (length). The small and the large pellets contain 0.7×10^{21} and 2.0×10^{21} atoms. Steep density gradients first developed in a zone inside q=1. Sawteeth were suppressed for one second and the energy confinement time was enhanced by up to 40 % over that of gas fuelled plasmas at a medium neutral beam heating power up to 15 MW[1]. The improved discharges are characterized by a strongly peaked pressure profile around the magnetic axis (inside the sawtooth inversion radius) and degrades when a large sawtooth occurs or when the pressure gradient reaches a critical value[6].

Figure 1-b) and -c) show the temporal evolution of Ti XIX, XX and XXI emissivity lines measured by crystal spectroscopy in the pellet fueled plasma. The line density at half the plasma radius, central electron temperature and the central soft X-ray signal are also shown in Fig. 1-a) and -b), respectively. The four hydrogen ice pellets are injected at around 6.0 sec into the helium discharge with $I_p = 3.1$ MA and $B_t = 4.8$ T. The combination of pellet sizes is two 2.7 ϕ and two 3.8 ϕ. The typical time interval adopted for each pellet is 50 msec, and the pellets are injected at low heating power of 7 MW to avoid the ablation due to beam fast ions. The NB heating power increases up to 15 MW

$$= n_k D_k^{NC} \left[- L_k \frac{n_k'}{n_k} + H_k \frac{T_k'}{T_k} + \frac{eZ_k}{T_k} \sum Z_j D_j n_j \left\{ L_j \frac{n_j'}{n_j} - H_j \frac{T_j'}{T_j} \right\} / \sum \frac{eZ_j^2 D_j n_j}{T_j} \right] \tag{15}$$

where $D_k^{NC} = (\frac{1}{2} + q^2) \rho_k^2 \sum_{j \neq k} \nu_{kj}$.

Using the above combination of neoclassical and anomalous transport fluxes, a one-dimensional and time dependent, multi-species impurity code[5] is employed to calculate the impurity ion density and the emissivity lines, in pellet fueled plasmas.

3. Intrinsic titanium impurity behavior in pellet fueled plasmas

Centrally peaked electron density profiles lasting for one second were obtained by injection of four hydrogen pellets into JT-60 neutral beam heated discharges. A four-barrel pneumatic pellet injector installed on JT-60 produces cylindrical hydrogen pellets with velocities approaching 1.6 km/s. The pellet sizes are 2.7 mm (dia.) × 2.7 mm (length) and 3.8 mm (dia.) × 3.8 mm (length). The small and the large pellets contain 0.7×10^{21} and 2.0×10^{21} atoms. Steep density gradients first developed in a zone inside q=1. Sawteeth were suppressed for one second and the energy confinement time was enhanced by up to 40 % over that of gas fuelled plasmas at a medium neutral beam heating power up to 15 MW[1]. The improved discharges are characterized by a strongly peaked pressure profile around the magnetic axis (inside the sawtooth inversion radius) and degrades when a large sawtooth occurs or when the pressure gradient reaches a critical value[6].

Figure 1-b) and -c) show the temporal evolution of Ti XIX, XX and XXI emissivity lines measured by crystal spectroscopy in the pellet fueled plasma. The line density at half the plasma radius, central electron temperature and the central soft X-ray signal are also shown in Fig. 1-a) and -b), respectively. The four hydrogen ice pellets are injected at around 6.0 sec into the helium discharge with $I_p = 3.1$ MA and $B_t = 4.8$ T. The combination of pellet sizes is two 2.7 ϕ and two 3.8 ϕ. The typical time interval adopted for each pellet is 50 msec, and the pellets are injected at low heating power of 7 MW to avoid the ablation due to beam fast ions. The NB heating power increases up to 15 MW

after the pellet injection. The intensities of Ti XIX and Ti XX rapidly increase due to the sudden reduction of the electron temperature by pellet injection. Conversely, the intensity of Ti XXI decreases at once and comes back to increase until the reappearance of a sawtooth at ~7.05 sec. The central soft X-ray signal also shows the same behavior as the temporal evolution of Ti XXI. Figure 2 shows the temporal evolutions of the profiles of electron density and electron temperature of a pellet fueled plasma. The electron density abruptly increases due to the pellet injections at around 6.0 sec, and the density profile seems to shrink later and is relaxed at 7.05 sec by the reappearance of sawtooth oscillation. The fundamental question is whether the titanium impurity accumulates or not in pellet fuelled plasmas showing improved confinement. Because plasma profiles dynamically change as shown in Fig. 2, there is still a possibility to explain the temporal evolutions of Ti intensity from the changes of electron temperature and density profiles in time and space.

4. Unsteady impurity transport analysis

First, we present calculations of the anomalous predicted time behavior of intrinsic Ti-impurity in the pellet fueled plasma with the profiles of the electron density and the electron temperature shown in Fig. 2. This calculation was performed for comparison with time evolutions of Ti XX and Ti XXI emissivity lines observed after pellet fuelling. Our interest will be limited to the range up to 7.0 sec, because the sawtooth dominated transport is beyond our scope.

Figure 3 shows the comparison of the observed line emissivities with the calculated time evolutions of Ti XX and Ti XXI, for systematic parameter scans of C_V from 1 to 4. The measured and calculated values are normalized to the values before the pellet injection. The calculated temporal evolution of Ti XXI needs a larger value of C_V in order to meet the observation. The result of Ti XX, however, reveals that the peaking parameter must be less than two. These results indicate that the contribution of the conventional diffusive/convective transport model is eventually very unsuccessful in explaining the observed response of line emissivities to density and temperature profile changes.

after the pellet injection. The intensities of Ti XIX and Ti XX rapidly increase due to the sudden reduction of the electron temperature by pellet injection. Conversely, the intensity of Ti XXI decreases at once and comes back to increase until the reappearance of a sawtooth at ~7.05 sec. The central soft X-ray signal also shows the same behavior as the temporal evolution of Ti XXI. Figure 2 shows the temporal evolutions of the profiles of electron density and electron temperature of a pellet fueled plasma. The electron density abruptly increases due to the pellet injections at around 6.0 sec, and the density profile seems to shrink later and is relaxed at 7.05 sec by the reappearance of sawtooth oscillation. The fundamental question is whether the titanium impurity accumulates or not in pellet fuelled plasmas showing improved confinement. Because plasma profiles dynamically change as shown in Fig. 2, there is still a possibility to explain the temporal evolutions of Ti intensity from the changes of electron temperature and density profiles in time and space.

4. Unsteady impurity transport analysis

First, we present calculations of the anomalous predicted time behavior of intrinsic Ti-impurity in the pellet fueled plasma with the profiles of the electron density and the electron temperature shown in Fig. 2. This calculation was performed for comparison with time evolutions of Ti XX and Ti XXI emissivity lines observed after pellet fuelling. Our interest will be limited to the range up to 7.0 sec, because the sawtooth dominated transport is beyond our scope.

Figure 3 shows the comparison of the observed line emissivities with the calculated time evolutions of Ti XX and Ti XXI, for systematic parameter scans of C_V from 1 to 4. The measured and calculated values are normalized to the values before the pellet injection. The calculated temporal evolution of Ti XXI needs a larger value of C_V in order to meet the observation. The result of Ti XX, however, reveals that the peaking parameter must be less than two. These results indicate that the contribution of the conventional diffusive/convective transport model is eventually very unsuccessful in explaining the observed response of line emissivities to density and temperature profile changes.

This situation is reminiscent of the neoclassical transport that provides impurity accumulation due to large density gradients through the electron density evolution in pellet fueled plasmas as shown in Fig. 1. Although impurity collisionality in pellet fueled plasmas lies in the Pfirsch-Schluter regime, the temperature screening effect driven by the temperature gradient term could not play the role to prevent the impurity accumulation, because of the flat temperature profile. Accordingly, the nature of profiles in pellet fueled plasmas strongly encourages impurity accumulation. The combination of the anomalous transport and neoclassical transport models is now examined. In Fig. 4, comparison of measured emissivity lines with simulation results based on neoclassical transport theory demonstrates that the contribution of neoclassical flux is at least an order of magnitude smaller than the anomalous transport flux. Accordingly, the simple combination of anomalous and neoclassical transport fluxes cannot account for the observed response of line emissivities.

Returning to the individual behavior of titanium impurities and soft X-ray signals, it is certainly found that the temporal evolution of Ti XXI is correlated with the duration of disappearing sawtooth oscillation. Concerning the effect of the sawtooth oscillation on impurity transport, some experiments have reported a continuous increase in the central soft X-ray emission followed by a rapid decrease with large m/n=1 MHD oscillations[7]. These results indicate improvement of central confinement in the sawtooth free phase. We therefore propose a two zone model as shown in Fig. 5; the inner plasma zone with reduced transport extending to the q=1 surface, and the outer plasma zone continuing to be dominated by anomalous transport. As for reduced transport, the anomalous diffusion coefficient in the inner zone is assumed to be a factor of ten smaller than that in the outer zone. Figure 6 shows the behavior of TI XXI and XX emissivity lines simulated by the two-zone model. The predicted titanium evolutions are in good agreement with observation. Therefore, impurity transport appears to be reduced to a level close to neoclassical in the

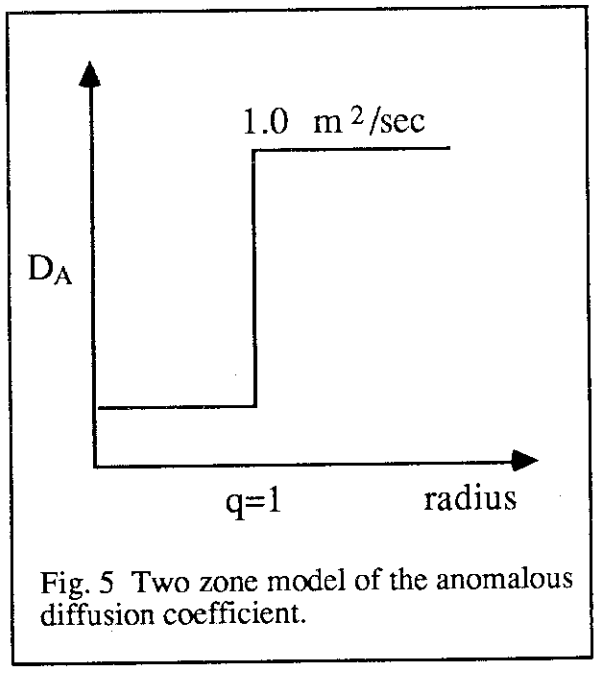

Fig. 5 Two zone model of the anomalous diffusion coefficient.

central good confinement region of in pellet fuelled discharges.

On the other hand, we also have to pay attention to another aspect of the neoclassical impurity transport theory which predicts enhanced, inward transport particle flux due to collisions with light impurity ions. In our pellet experiments, it has been reported that the light impurity contents of carbon and oxygen were 3 % and 1 %, respectively, before the pellet injection[8]. The effects of light impurities on titanium impurity transport is not small. Since the Ti flux is driven largely by the C and O ions, it is necessary to properly take into account the interaction with the C and O ions. Including the contribution of light-heavy impurity collisions to impurity ion fluxes, we calculated the titanium impurity ion behavior and presented the results in Fig. 7 for scanned parameters of reduced anomalous diffusion coefficients from $0.1m^2/s$ to $0.3m^2/s$. Holding $D_A = 0.1m^2/s$, the calculated results show stronger impurity accumulation due to the collisions between light and titanium impurity ions, and are not in agreement with the experimental observations. If the outward flux driven by anomalous diffusion in the improved confinement region still prevents the impurity accumulation predicted by the neoclassical transport theory, one could estimate the value of the reduced anomalous diffusion coefficient so that the calculation results match the observed behavior. Then, it is found that the value of the anomalous diffusion coefficient is $0.2m^2/s$ in the central, improved confinement region.

5. Summary and discussion

Impurity transport analysis shows that the titanium impurity ions accumulate in the plasma core region, correlated with peaked density profile and the absence of sawtooth oscillation in a plasma deeply fueled by pellet. This impurity behavior is well described by the combination of reduced anomalous diffusion and neoclassical transport in the plasma interior. Impurity accumulation is caused by a strong ion density gradient driving force and collisions with light impurities, as the neoclassical impurity transport theory predicts. The reduced anomalous diffusion at the central region inside the q=1 surface is estimated to be 0.2 m^2/s. The outer zones continue to be dominated by anomalous transport.

The metal impurity accumulation, in general agreement with estimates of neoclassical transport, strongly suggests that an impurity problem is still one of the fatal problems in a

central good confinement region of in pellet fuelled discharges.

On the other hand, we also have to pay attention to another aspect of the neoclassical impurity transport theory which predicts enhanced, inward transport particle flux due to collisions with light impurity ions. In our pellet experiments, it has been reported that the light impurity contents of carbon and oxygen were 3 % and 1 %, respectively, before the pellet injection[8]. The effects of light impurities on titanium impurity transport is not small. Since the Ti flux is driven largely by the C and O ions, it is necessary to properly take into account the interaction with the C and O ions. Including the contribution of light-heavy impurity collisions to impurity ion fluxes, we calculated the titanium impurity ion behavior and presented the results in Fig. 7 for scanned parameters of reduced anomalous diffusion coefficients from $0.1m^2/s$ to $0.3m^2/s$. Holding $D_A = 0.1m^2/s$, the calculated results show stronger impurity accumulation due to the collisions between light and titanium impurity ions, and are not in agreement with the experimental observations. If the outward flux driven by anomalous diffusion in the improved confinement region still prevents the impurity accumulation predicted by the neoclassical transport theory, one could estimate the value of the reduced anomalous diffusion coefficient so that the calculation results match the observed behavior. Then, it is found that the value of the anomalous diffusion coefficient is $0.2m^2/s$ in the central, improved confinement region.

5. Summary and discussion

Impurity transport analysis shows that the titanium impurity ions accumulate in the plasma core region, correlated with peaked density profile and the absence of sawtooth oscillation in a plasma deeply fueled by pellet. This impurity behavior is well described by the combination of reduced anomalous diffusion and neoclassical transport in the plasma interior. Impurity accumulation is caused by a strong ion density gradient driving force and collisions with light impurities, as the neoclassical impurity transport theory predicts. The reduced anomalous diffusion at the central region inside the q=1 surface is estimated to be 0.2 m^2/s. The outer zones continue to be dominated by anomalous transport.

The metal impurity accumulation, in general agreement with estimates of neoclassical transport, strongly suggests that an impurity problem is still one of the fatal problems in a

future reactor. In a fusion plasma, it is assumed that the central ion temperature should be higher than 33 keV and the central density larger than 1.05×10^{20} m^{-3}. Since a reactor plasma radius is only a factor of 2 larger than that of present tokamak devices, the gradients of temperature and density become large. Accordingly, the impurity particle fluxes driven by those gradient terms also can be estimated to be large. Furthermore, the impurity ion collision frequency enters the plateau or banana regions in such fusion plasmas with temperature as high as 33 keV. In such a collision regime, the ion temperature gradient term does not work any more as a temperature screening effect but as an inward driving force, resulting in impurity accumulation. In a design study for a fusion reactor, it is also recognized that the sawtooth suppression is one of the key issues in obtaining a reactor plasma. Therefore, the profile characteristics assumed for a fusion plasma may cause impurity accumulation. This indicates the need for active impurity control research.

Acknowledgment

We are indebted to the entire JT-60 team and in particular to the diagnostics and data management groups for providing the basic data for this study. A critical reading of the manuscript by D. Humphreys is appreciated.

References

[1] KAMADA, Y., YOSHINO, R., NAGAMI, M., et al., Nucl. Fusion **29** (1989) 1785.

[2] COPPI, B., SHARKY, N., Proc. of the Course on Physics of Plasmas close to Thermonuclear Conditions, EUR FU BRU/XII/476/80, (Varenna, 1979), 47.

[3] KOIDE, Y., HIRAYAMA, T., SUGIE, T., et al., Nucl. Fusion **28** (1988) 1835.

[4] SAMAIN, A., WERKOFF, F., Nucl. Fus. **17** (1977) 53.

[5] HIRAYAMA, T., SHIRAI, H., SHIMIZU, K., et al., J. Nucl. Materials, **145-147** (1987) 145.

[6] OZEKI, T., AZUMI, M., KAMADA, Y., et al., Nucl. Fusion **31** (1991) 51.

[7] Doublet III Group, J. Nucl. Mater. **93&94** (1980) 2509.

[8] SUGIE, T., KUBO, H., SAKASAI, A., et al., Proc. 17th Int. Conf. on Plasma Physics and Controlled Nucl. Fusion Research, (Amsterdam, 1990) Vol.1 223.

future reactor. In a fusion plasma, it is assumed that the central ion temperature should be higher than 33 keV and the central density larger than 1.05×10^{20} m^{-3}. Since a reactor plasma radius is only a factor of 2 larger than that of present tokamak devices, the gradients of temperature and density become large. Accordingly, the impurity particle fluxes driven by those gradient terms also can be estimated to be large. Furthermore, the impurity ion collision frequency enters the plateau or banana regions in such fusion plasmas with temperature as high as 33 keV. In such a collision regime, the ion temperature gradient term does not work any more as a temperature screening effect but as an inward driving force, resulting in impurity accumulation. In a design study for a fusion reactor, it is also recognized that the sawtooth suppression is one of the key issues in obtaining a reactor plasma. Therefore, the profile characteristics assumed for a fusion plasma may cause impurity accumulation. This indicates the need for active impurity control research.

Acknowledgment

We are indebted to the entire JT-60 team and in particular to the diagnostics and data management groups for providing the basic data for this study. A critical reading of the manuscript by D. Humphreys is appreciated.

References

[1] KAMADA, Y., YOSHINO, R., NAGAMI, M., et al., Nucl. Fusion **29** (1989) 1785.

[2] COPPI, B., SHARKY, N., Proc. of the Course on Physics of Plasmas close to Thermonuclear Conditions, EUR FU BRU/XII/476/80, (Varenna, 1979), 47.

[3] KOIDE, Y., HIRAYAMA, T., SUGIE, T., et al., Nucl. Fusion **28** (1988) 1835.

[4] SAMAIN, A., WERKOFF, F., Nucl. Fus. **17** (1977) 53.

[5] HIRAYAMA, T., SHIRAI, H., SHIMIZU, K., et al., J. Nucl. Materials, **145-147** (1987) 145.

[6] OZEKI, T., AZUMI, M., KAMADA, Y., et al., Nucl. Fusion **31** (1991) 51.

[7] Doublet III Group, J. Nucl. Mater. **93&94** (1980) 2509.

[8] SUGIE, T., KUBO, H., SAKASAI, A., et al., Proc. 17th Int. Conf. on Plasma Physics and Controlled Nucl. Fusion Research, (Amsterdam, 1990) Vol.1 223.

future reactor. In a fusion plasma, it is assumed that the central ion temperature should be higher than 33 keV and the central density larger than 1.05×10^{20} m^{-3}. Since a reactor plasma radius is only a factor of 2 larger than that of present tokamak devices, the gradients of temperature and density become large. Accordingly, the impurity particle fluxes driven by those gradient terms also can be estimated to be large. Furthermore, the impurity ion collision frequency enters the plateau or banana regions in such fusion plasmas with temperature as high as 33 keV. In such a collision regime, the ion temperature gradient term does not work any more as a temperature screening effect but as an inward driving force, resulting in impurity accumulation. In a design study for a fusion reactor, it is also recognized that the sawtooth suppression is one of the key issues in obtaining a reactor plasma. Therefore, the profile characteristics assumed for a fusion plasma may cause impurity accumulation. This indicates the need for active impurity control research.

Acknowledgment

We are indebted to the entire JT-60 team and in particular to the diagnostics and data management groups for providing the basic data for this study. A critical reading of the manuscript by D. Humphreys is appreciated.

References

[1] KAMADA, Y., YOSHINO, R., NAGAMI, M., et al., Nucl. Fusion **29** (1989) 1785.

[2] COPPI, B., SHARKY, N., Proc. of the Course on Physics of Plasmas close to Thermonuclear Conditions, EUR FU BRU/XII/476/80, (Varenna, 1979), 47.

[3] KOIDE, Y., HIRAYAMA, T., SUGIE, T., et al., Nucl. Fusion **28** (1988) 1835.

[4] SAMAIN, A., WERKOFF, F., Nucl. Fus. **17** (1977) 53.

[5] HIRAYAMA, T., SHIRAI, H., SHIMIZU, K., et al., J. Nucl. Materials, **145-147** (1987) 145.

[6] OZEKI, T., AZUMI, M., KAMADA, Y., et al., Nucl. Fusion **31** (1991) 51.

[7] Doublet III Group, J. Nucl. Mater. **93&94** (1980) 2509.

[8] SUGIE, T., KUBO, H., SAKASAI, A., et al., Proc. 17th Int. Conf. on Plasma Physics and Controlled Nucl. Fusion Research, (Amsterdam, 1990) Vol.1 223.

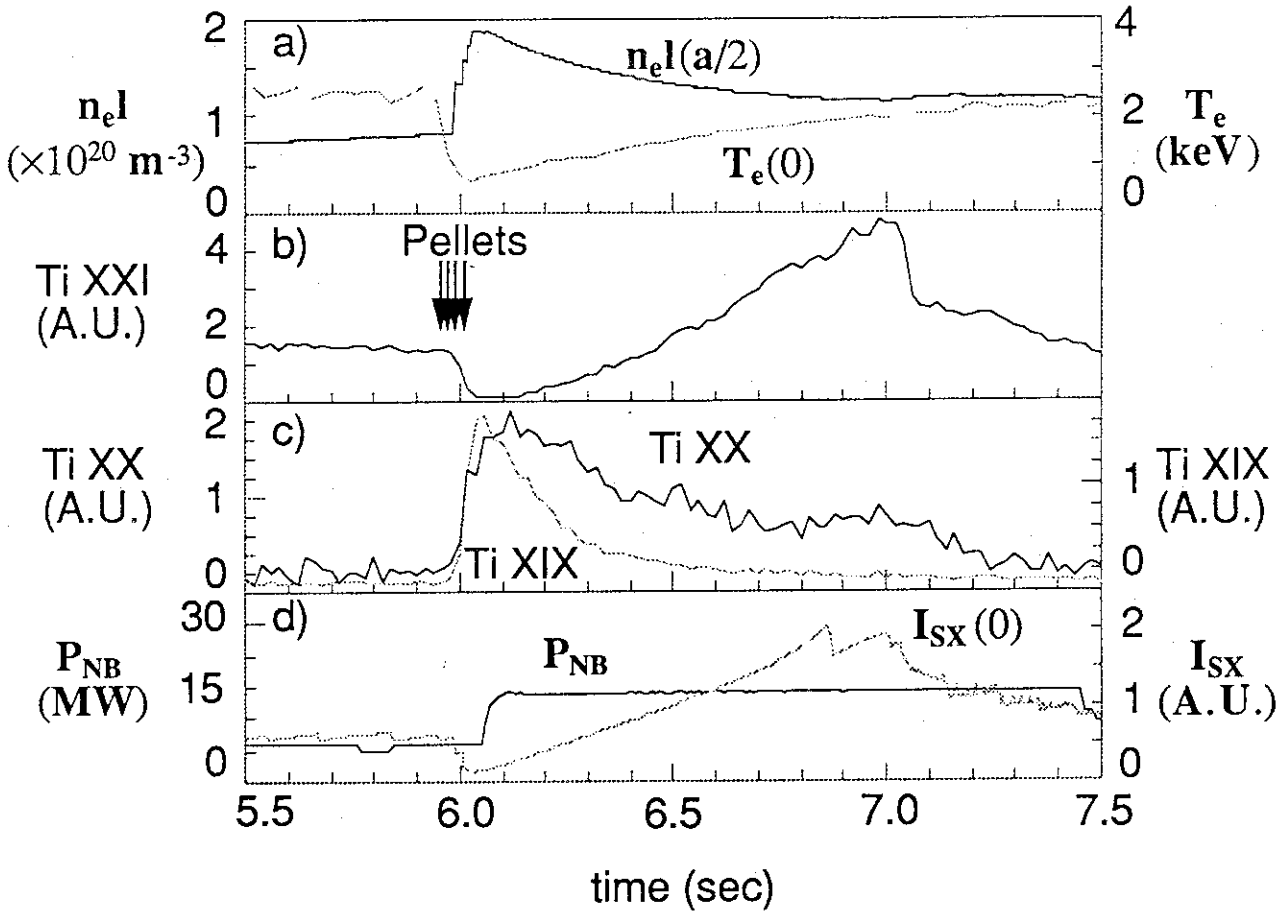

Fig. 1 Temporal behaviors of plasma parameters of a pellet fueled plasma: a) the line electron density $n_e l$ at about half the plasma radius and the central electron temperature T_e ; b) the Ti XXI emissivity line ; c) the emissivity lines of Ti XX and Ti XIX ; d) the NB heating power, P_{NB}, and the central soft X-ray intensity, I_{SX}.

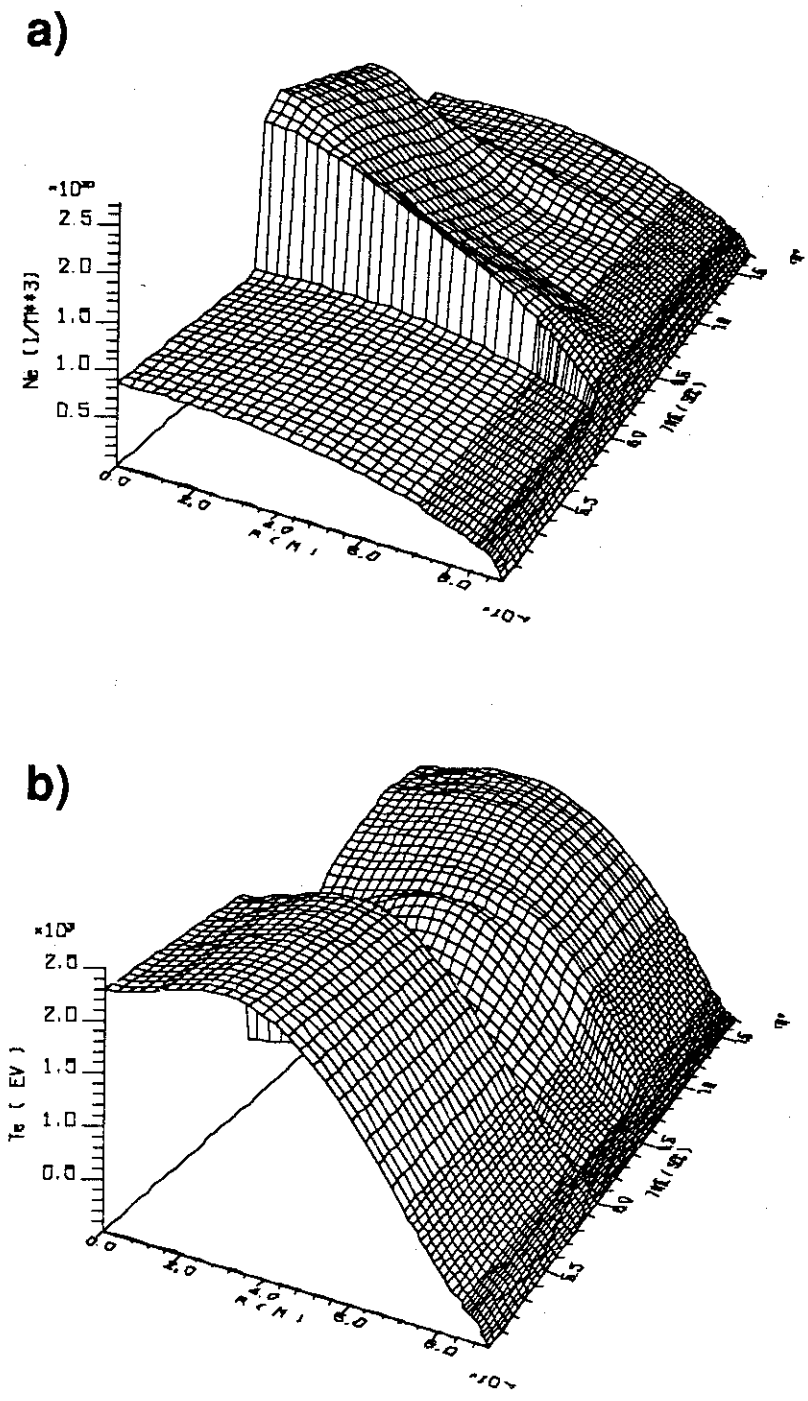

Fig. 2 Time evolutions of a) the electron density profile, and b) the electron temperature profile.

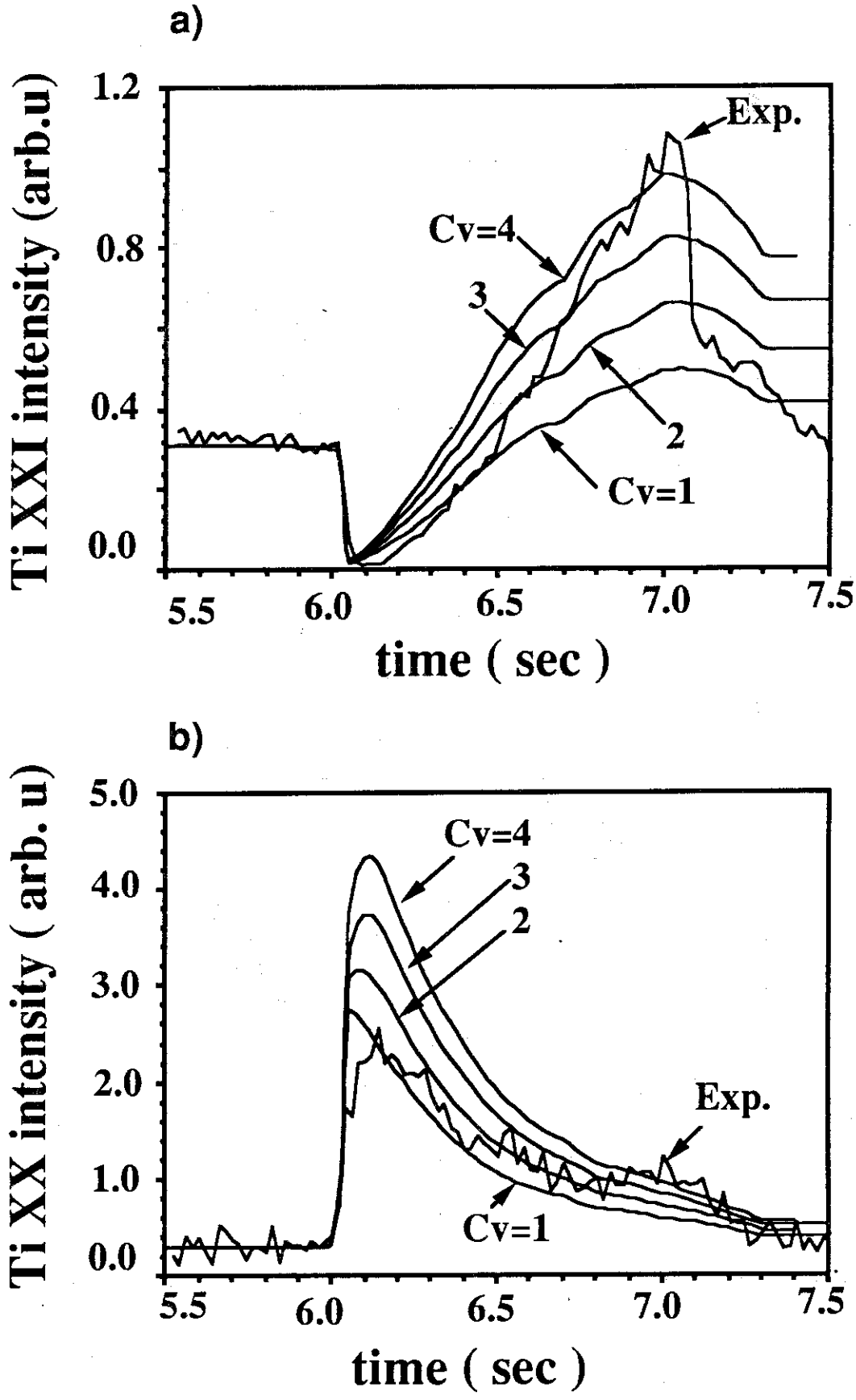

Fig. 3 Comparison of measured emissivity lines with simulation results for scanning Cv from 1 to 4, holding the uniform D_A = 1.0 m^2/s: a) Ti XXI ; b) Ti XX.

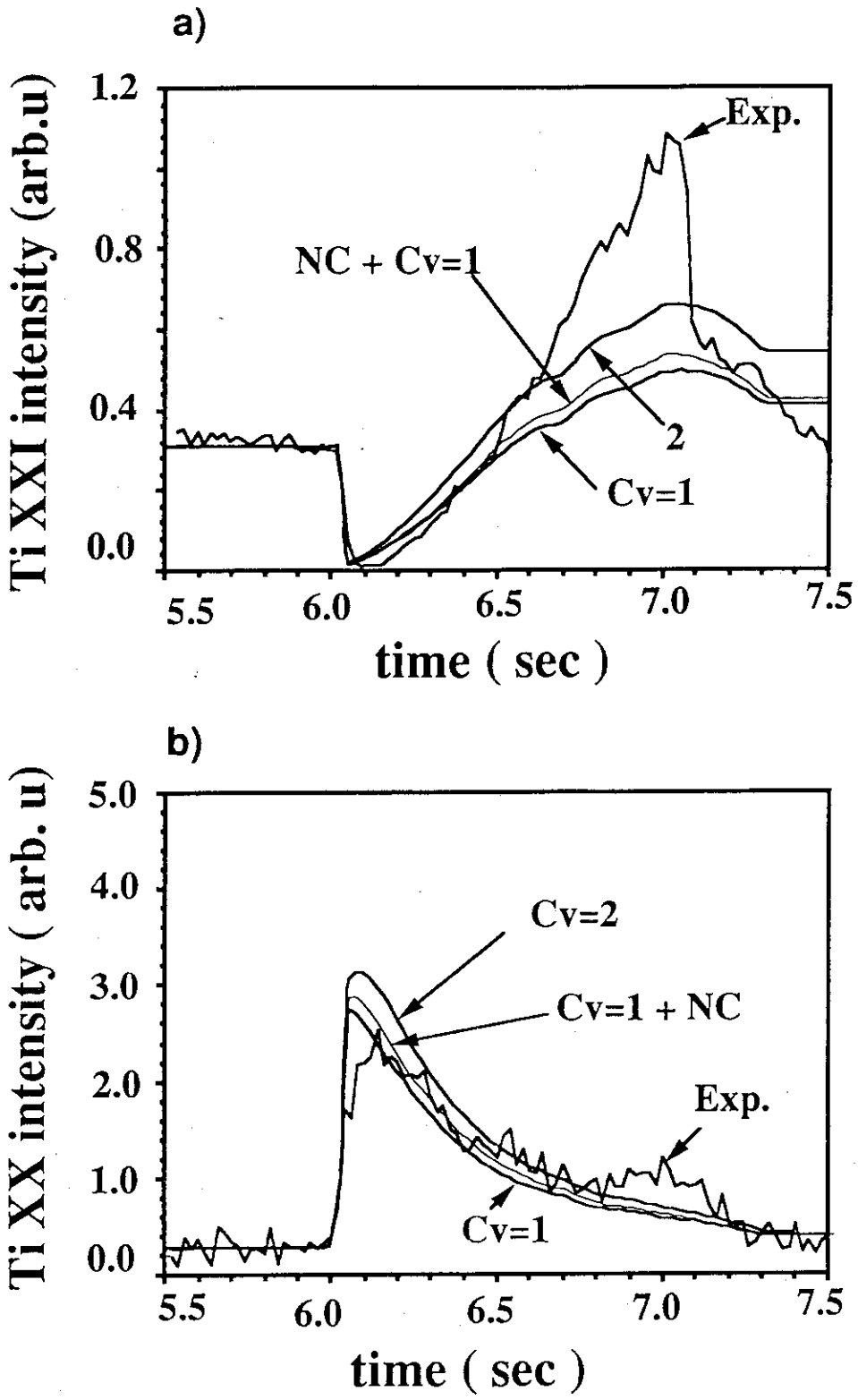

Fig. 4 Temporal behavior of the emissivity lines of a) Ti XXI, and b) Ti XX calculated by taking the neoclassical impurity transport flux into the anomalous transport driven flux with the uniform $D_A = 1.0\ m^2/s$.

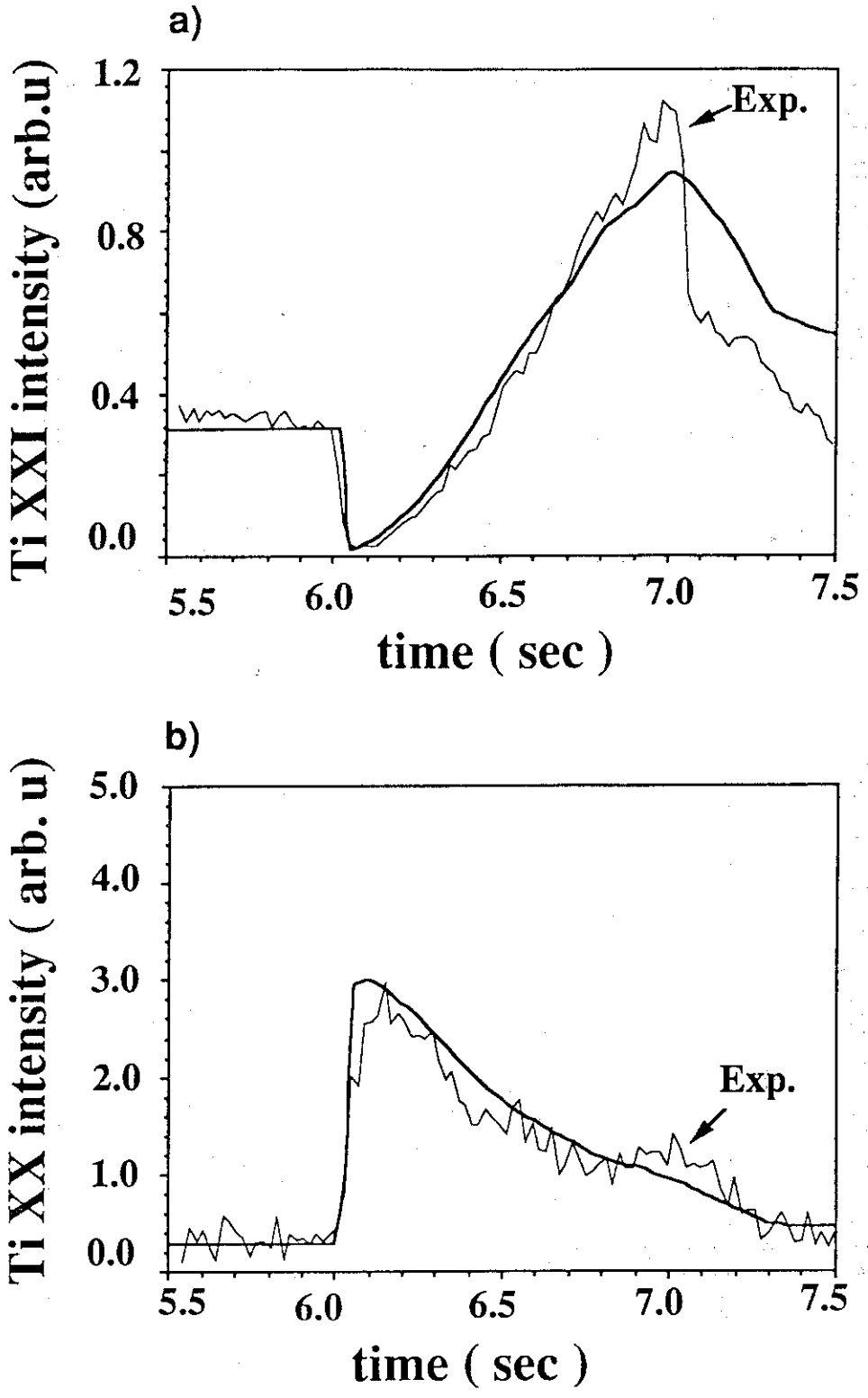

Fig. 6 Comparison of measured lines with the simulation results based on the two zone model assuming the improved transport inside the q=1 surface : a) Ti XXI ; b) Ti XX.

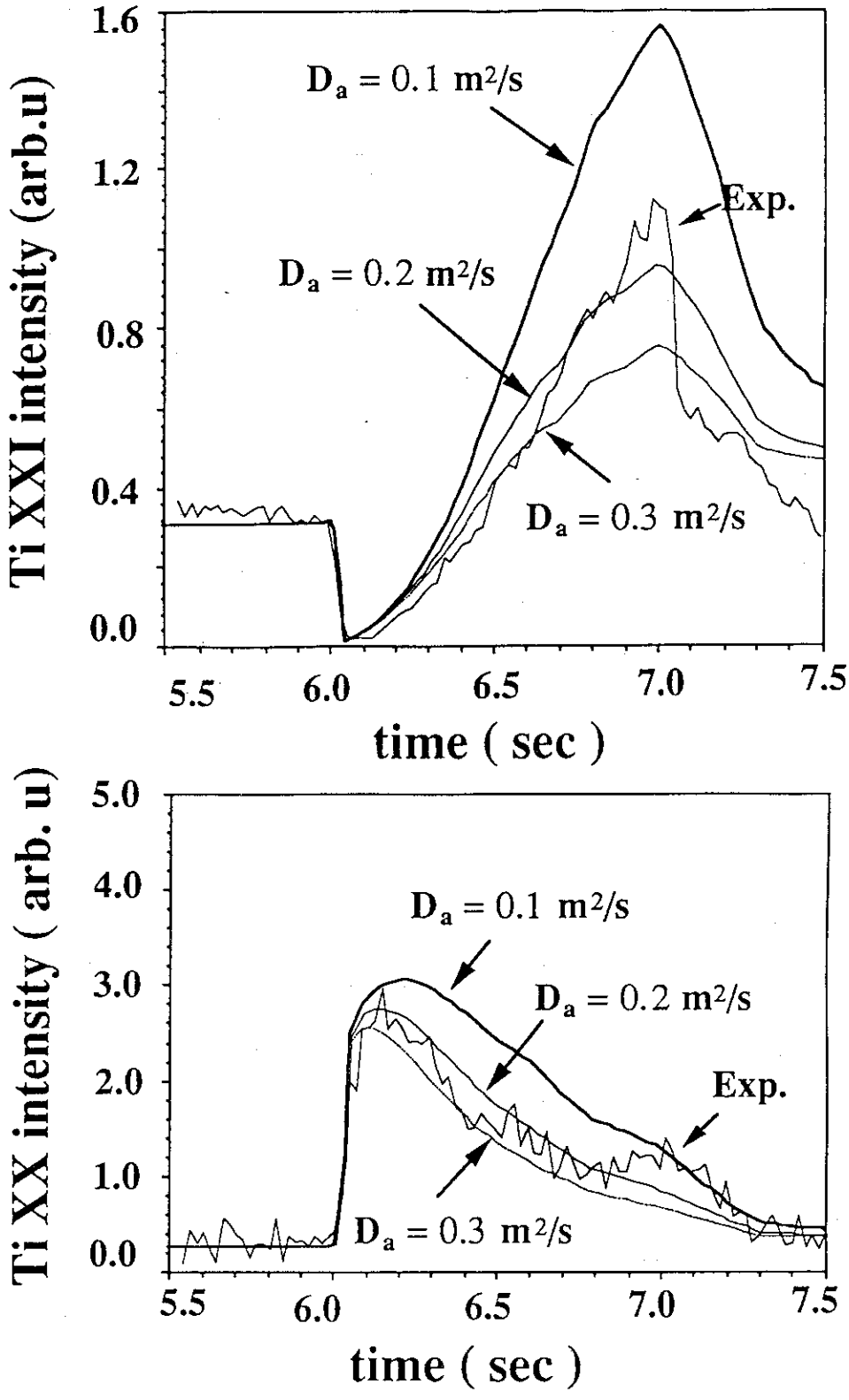

Fig. 7 Comparison of measured lines with the simulation results for scanned parameters of reduced anomalous diffusion coefficients from 0.1 m^2/s to 0.3 m^2/s inside the q=1 surface : a) Ti XXI ; b) Ti XX.